

From mass-wasting to slope stabilization – putting constraints on a tectonically induced transition in slope erosion mode: a case study in the Judea Hills, Israel

Uri Ryb,^{1*} Ari Matmon,¹ Naomi Porat² and Oded Katz²

¹ The Fredy and Nadine Herrmann institute of Earth Sciences, The Hebrew University, Jerusalem, Israel

² Geological Survey of Israel, Jerusalem, Israel

Received 14 September 2011; Revised 18 June 2012; Accepted 20 June 2012

*Correspondence to: Uri Ryb, The Fredy and Nadine Herrmann institute of Earth Sciences, Admond J. Safra Campus, Givat Ram, Jerusalem, 91904, Israel. Email: uri.ryb@mail.huji.ac.il

ESPL

Earth Surface Processes and Landforms

ABSTRACT: Calcrete-coated remnants of landslide debris and alluvial deposits are exposed along the presently stable hillslopes of the Soreq drainage, Judea Hills, Israel. These remnants indicate that a transition from landslide-dominated terrain to dissolution-controlled hillslope erosion had occurred. This transition possibly occurred due to the significant decrease in tectonic uplift during the late Cenozoic. The study area is characterized by sub-humid Mediterranean climate. The drainage hillslopes are typically mantled by thick calcrete crusts overlying Upper Cretaceous marine carbonate rocks. Using TT-OSL dating of aeolian quartz grains incorporated in the calcrete which cements an ancient landslide deposit, we conclude that incision of ~100 m occurred from 1056 ± 262 to 688 ± 86 ka due to ~0.3° westward tilt of the region; such incision invoked high frequency of landslide activity in the drainage. The ages of a younger landslide remnant, alluvial terrace, and alluvial fan, all situated only a few meters above the present level of the active streambed, range between 688 ± 86 ka and 244 ± 25 ka and indicate that since 688 ± 86 the Soreq base level had stabilized and that landslide activity decreased significantly by the middle Pleistocene. Copyright © 2012 John Wiley & Sons, Ltd.

KEYWORDS: hillslope transport; carbonate terrains; TT-OSL; erosion mode; calcrete

Introduction

Erosion of hillslopes occurs by discrete mass wasting events such as landslides and debris-flow, and through gradual diffusive processes such as soil creep and rock dissolution (Burbank *et al.*, 1996; Bloom, 1998; Roering *et al.*, 2001; Heimsath *et al.*, 2002). Diffusive processes act on various slope gradients while landslides require a minimal critical slope gradient which may vary according to the strength of the substrate. Slope failure could be triggered by the removal of material from the toe of the hillslope (Bigi *et al.*, 2006), increase in the pore pressure during extreme rainfall (Iverson, 2000), ground-acceleration during an earthquake (Keefer, 1994), and loss of vegetation cover due to human activity, grazing, or wildfire (e.g. Wondzell and King, 2003). After slope-failure debris is deposited at the angle of repose and the slope stabilizes. Base-level lowering maintains critical slopes and enables a continuous erosion of a region through landsliding. Therefore, landslides are a common erosive process in tectonically uplifting mountains with high-relief (Burbank *et al.*, 1996; Hovius, 1998; Frankel and Pazzaglia, 2006). Compared to diffusive processes, hillslope erosion through landsliding dramatically increases the sediment flux to the alluvial network

and the overall drainage erosion. Researchers observe an increase in sediment flux in response to landsliding in the tectonically active Olympic Mountains, Washington, using fission-track thermochronometry (Montgomery and Brandon, 2002), and in San Bernardino Mountains, California (Binnie *et al.*, 2007) and the Icacos River, Puerto Rico (Brown *et al.*, 1995) using cosmogenic isotopes concentrations in sediment. Measuring erosion-rates over different timescales at the mountains of central Idaho, Kirchner *et al.* (2001) found dramatic variations which were attributed to temporal transition in the region's hillslope mode of erosion.

Conversely, during a transition from landslide to diffusion controlled hillslope erosion, the flux of coarse sediments decreases significantly. As a result one should expect the accumulation of high volumes of alluvial and colluvial deposits to be associated with periods of landslide-controlled hillslope erosion, and lower volumes (or absence of deposits) associated with periods of slope stability. This difference is expected to be most pronounced in carbonate terrains; carbonate rocks in non-arid climates tend to diffuse through dissolution. Therefore, periods of stable hillslopes are expected to be associated with very low coarse-sediment flux, and respectively, degradation of existing alluvial and colluvial sediment deposits.

In such terrains transitions between discrete and diffusive modes of hillslope erosion translate to periods of alluvial and colluvial deposit buildup or destruction, respectively.

In the current paper we discuss the driving mechanism and the duration of a transition in hillslope mode of erosion in the Judea Hills, Israel. Contrary to previous studies that are based on variations in basin-scale erosion rates, here we present new field observations and chronological data of alluvial and colluvial deposits that mark different base levels and which can be associated with different frequencies of landslides. We then use the dates to constrain the drainage-scale geomorphic response time to a pause in tectonic uplift. The methods and reasoning we applied here can be used in other locations to trace phases of tectonic activity or quiescence through the geomorphic response of hillslopes.

Study Area and Geological Settings

The mountainous backbone of Israel rises up to ~1000 m above sea level between the Mediterranean and the Dead Sea base levels (Figure 1). This range is mostly composed of Albian-Turonian marine carbonate rocks (dolomite, limestone, and marl), flanked by Senonian softer units (mostly chalk and marl) (Bentor *et al.*, 1965). The topography of the range follows a fold structure composed of short wavelength (10–20 km) asymmetrical folds superimposed on a long wavelength (~70 km) structural arch which developed as a marginal response to the subsidence of the Dead Sea Rift (DSR) (Wdowinski and Zilberman, 1996, 1997) since the late Neogene.

Our study focuses on the central part of the range, also known as the Judea Hills (Figure 1). In contrast to the fairly known Mesozoic and early Cenozoic geologic history (e.g. Saas and Bein, 1978), the stages of mountain uplift, the emergence of the Judea Hills above the sea, and the erosion that accompanied the uplift remain mostly unknown. Partly, because correlative and datable deposits that may assist in reconstructing landscape evolution are rare and were not investigated. Nevertheless, it is widely agreed that the uplift of the mountainous backbone in central Israel began during the Miocene (Sneh and Buchbinder, 1984; Begin and Zilberman, 1997). Buchbinder *et al.* (2005) claim that the uplift started earlier in the Oligocene, based on the incision of canyons in the coastal plain during that period. Bar (2009) suggested that the greater part of the uplift of the Judea Range occurred in two pulses: during early Miocene (~500 m of vertical uplift without regional tilting or short-wave folding) and in the late Pliocene (~300 m uplift, due to activation of the large scale structural arch and westward tilting of the region). Nevertheless, the stages at which the drainage systems developed as a response to Judea Hills uplift are even less understood in spite of some early studies (e.g. Shatner, 1957; Nir, 1989), mainly due to the lack of 'classical' datable markers such as volcanic rocks.

The major drainage of the Judea Hills is the Soreq (Figure 1). The Soreq drains the central ridge westward to the Mediterranean and extends over an area of ~760 km². The drainage is divided into a mountainous segment (800–250 m above sea level) and the piedmont (250–0 m above sea level). In its mountainous segment, the Soreq incises some 400 m below the Judea Hills highland through Cretaceous marine carbonate rocks. The

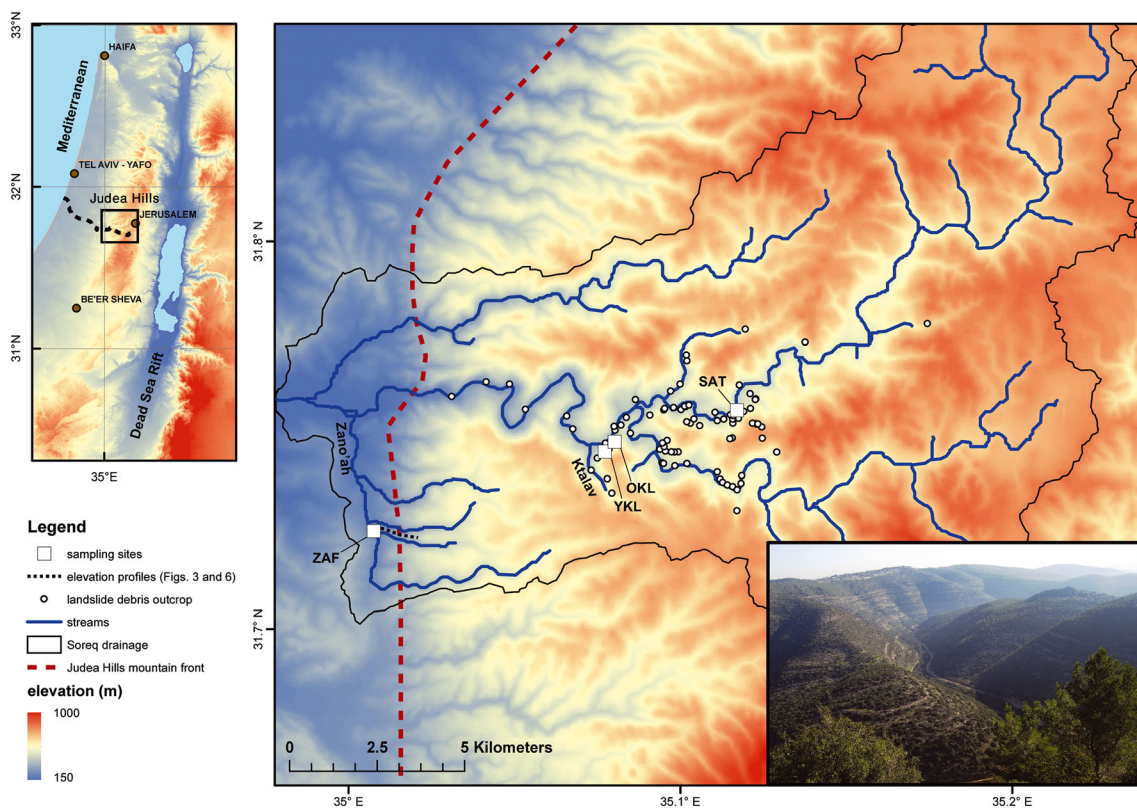


Figure 1. Digital elevation model (DEM) map of the Soreq drainage system. Dashed red line delineates the Judea Hills mountain front. White dots mark the center of single-landslide outcrops. Sampling sites are labeled according to the order of description in the text: 1, 'Young' Ktlav landslide (YKL); 2, 'Old' Ktlav landslide (OKL); 3, Zano'ah alluvial fan (ZAF); 4, Alluvial terrace at the main Soreq stem (SAT). Locations of topographic profiles of Figures 3 and 6 are marked with dashed lines in the main frame and inset, respectively. Photograph in the lower right inset shows the typical steep hillslopes of the Soreq drainage system. The photograph was taken west of the Soreq-Ktlav confluence (35.067°E/31.744°N); elevation difference from streambed to the interfluvium in the horizon is 300–400 m. Maps were plotted using Israel Transverse Mercator (ITM) projection. This figure is available in colour online at wileyonlinelibrary.com/journal/espl

drainage hillslopes are steep, and in many places exceed 30°. These slopes are typically mantled by massive calcrete crusts, which are common to the Mediterranean sub-humid climate (~500 mm and 18°C average annual precipitation and temperature, respectively, Ayalon *et al.*, 1998). Most runoff in the region occurs only after prolonged rain events indicating significant infiltration of water into the karstic system and the loss of water through small solution shafts along the thalwegs (Ford and Williams, 2007). In spite of the steepness, annual extreme rain-fall events, and rare earthquakes, no recent discrete mass-wasting events are evident (in the field or in aerial photographs) along the natural slopes of the Soreq drainage. Erosion of the slopes and interfluvies of the drainage is controlled by diffusive processes, mostly carbonate dissolution, and the sediment yield is low. Respectively, the Soreq and its tributaries are typically bedrock channels and no recent accumulation of alluvial sediments in fans and terraces occurs within the drainage system or along the Judea Hills mountain front.

Cenozoic Landslide Activity in the Soreq Drainage: Field Observations, Working Hypothesis, and Sampling Scheme

We revealed 84 landslide-debris outcrops in field and aerial photograph surveys of the Soreq drainage (Figure 1). The majority of landslide-debris outcrops were identified along road-cuts as their morphology and vegetation cover were indistinguishable from adjacent hillslopes. When exposed along a road cut, contacts between landslide-debris and the bedrock and, in places, between different generations of landslides, are clear (see figure DR1 in the online Supplementary Material). The outcrops appear mostly below the Albian section, which is characterized by thin beds of alternating dolomite and marl. All landslide debris and all alluvial sediments that were investigated in this study are cemented by mature calcretes (Figure 2c) (mostly stage V, Machette, 1985). Six landslides have a topographic expression and could be identified in an orthophoto (Figure 2a, see also figure DR2 in the online Supplementary Material). The 84 landslide-debris outcrops are derived from a potentially smaller number of landslides, since a single landslide may crop out in several locations at various elevations. Generally, two or more outcrops were considered to be of a single landslide if the following criteria applied: (a) the two outcrops were not separated by a spur or a ridge, and (b) one of the outcrops was found directly down-slope from the other or, in the case that the two outcrops are at the same level, are less than 50 m apart and are not separated by a clear contact. Using these criteria and including landslides that were visible in the orthophoto, we associate the outcrops with a minimum of 65 landslides. Most of the landslides (37 out of 65) were traced down to the present streambed or just slightly above it (< 10 m). The base-level of one landslide was identified ~100 m above the present streambed. The landslides coordinate and maximum base-level elevation above the present streambed is available in the online Supplementary Material, table DR3.

Working hypothesis, sites and sample descriptions

Our working hypothesis is that landslide material generally moves down slope all the way to the active streambed. Thus landslide-debris marks the upper-limit for the position of the active streambed at the time it occurred. The obvious lower-limit is the present streambed, as the Soreq mountainous

segment is a bedrock channel. Landslide-debris that crops out at, or within a few meters, of the present streambed must have occurred immediately after incision reached the present level and before diffusive processes had decreased hillslope gradients below the critical threshold. By focusing on the youngest alluvial and colluvial deposits we put temporal constraints on this transition. Ages of higher (older) deposits will help to constrain the rate of stream incision and, by inference, the rate of uplift in the past. Tectonic uplift potentially played a key role in the hillslope erosion mode transition. Our sampling strategy required samples from the youngest calcrete-coated debris deposits on the current base level and from deposits with known higher base level. Therefore, our selection was limited to four deposits with established base level. Other deposits in the Soreq drainage are poorly preserved (as expected in the dissolution-controlled terrain), and lack the morphologic features that indicate relative youngness or an established higher base level. Three deposits (two alluvial and one colluvial) are associated with the present streambed (< 4 m above it) and suggest insignificant incision since they were deposited; the fourth deposit (landslide-debris) overlies a conglomerate ~100 m above the present streambed, indicating significant incision since deposition. All selected deposits are cemented by stage V calcretes.

'Young' Ktalav landslide (YKL) (35.077°E/31.746°N)

The debris-cementing calcrete were sampled along a road-cut some 100 m above the Ktalav-Soreq confluence (Figure 1). This site was selected because the landslide exposed here has a noticeable scar, contrary to most landslides found in the Judea Hills, suggesting its relative young age; moreover, the debris extend all the way down to the active streambed (Figures 2a and 2b). The lower ~3 m of the calcrete outcrop contain large rock blocks (> 0.1 m diameter) which are overlain by a ~0.5 m thick calcrete with finer rock clasts (< 5 cm diameter) (Figure 2c). The transition between the coarse- and fine-clast calcretes is sharp, and could indicate that erosion occurred between two phases of colluvial sedimentation and calcretization. Three samples were collected from this outcrop, two from the coarse-clast calcrete (UR1 and UR2) and one from the fine-clast calcrete (UR3).

'Old' Ktalav landslide (OKL) (35.080°E/31.748°N)

A few hundred meters north of the 'Young' Ktalav landslide (YKL), the debris of a second landslide is exposed along the road cut. The debris, now cemented by thick (~4–5 m) calcrete, covers a rare conglomerate relict, some 100 m above the present streambed. Chert pebbles, included in the conglomerate, were derived from Senonian units which currently crop out only at the water divide, ~20 km to the east. The presence of these pebbles in the conglomerate indicates that it was deposited along the main Soreq stem. The preservation of the conglomerate bed on the steep slope (30°–40°) and the lack of calcrete-coated debris down slope of the outcrop (Figure 2d) suggest that the conglomerate was buried by the landslide shortly after its deposition. One sample was collected near the base of the landslide debris (UR4).

Alluvial fan adjacent to Wadi Zano'ah (ZAF) (35.007°E/31.726°N)

Two generations of alluvial fans were explored at Wadi Zano'ah, a tributary of the Soreq that runs along the mountain front (Figure 3). The relicts of the higher and older conglomerate are found coating the mountain front face up to 90 m above the current streambed; these relicts are entirely cemented by stage V hard-pan calcrete. The original morphology of the fan/terrace in which they were deposited has been eroded and a distinguished morphologic surface cannot be identified. The second and

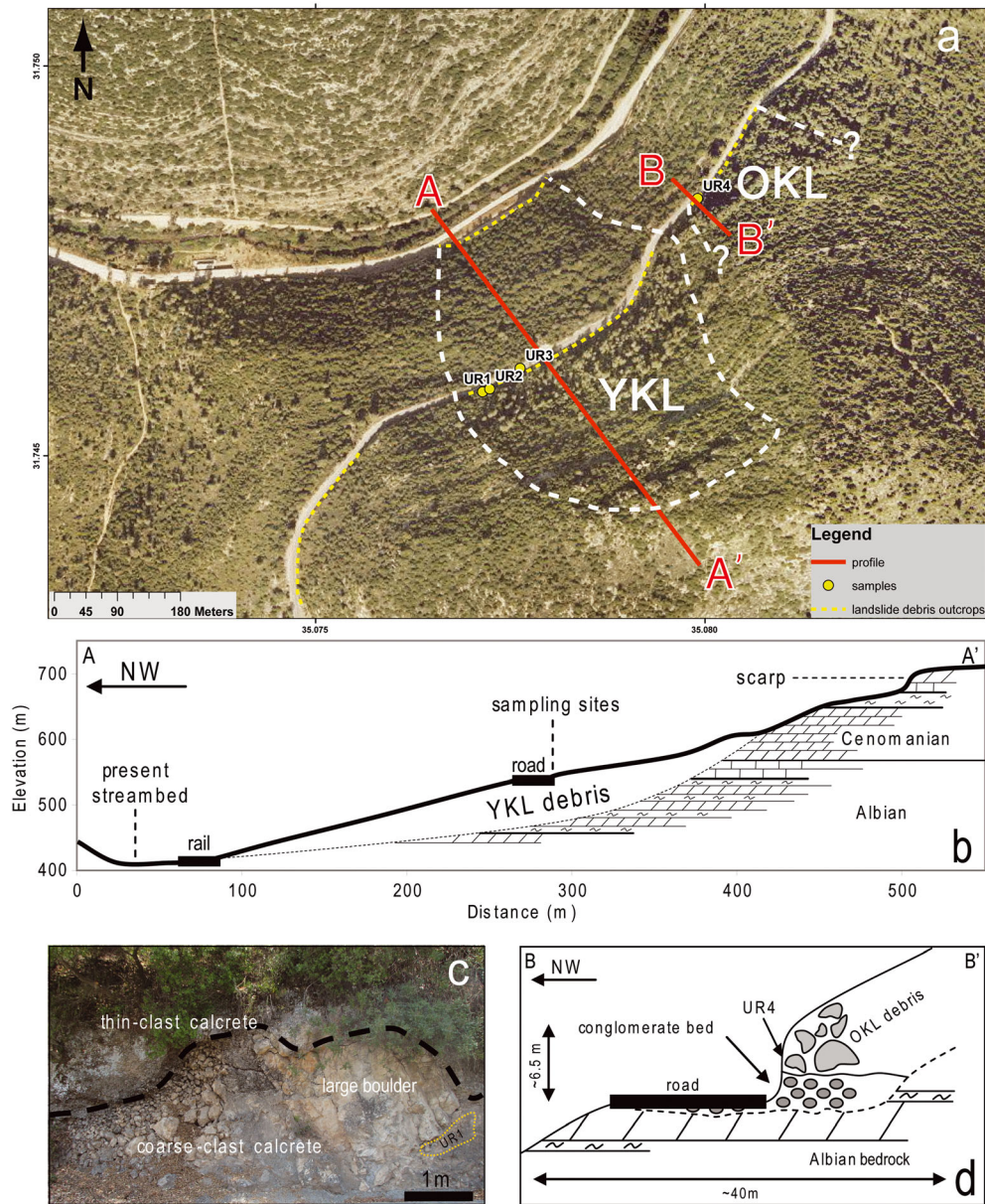


Figure 2. (a) Orthophoto of the 'Old' and 'Young' Ktalav landslides sites (OKL and YKL, respectively) and location of the optically stimulated luminescence (OSL) samples. The boundaries of the YKL are visible and a prominent scarp is found at the top of the landslide. OKL has no apparent topographic expression. Its debris is exposed only along the road cut. (b) Cross-section through the YKL (marked A–A' on the orthophoto), the scarp is clearly visible at the top of the slope, additional photograph of the scarp can be found in the online Supplementary Material, figure DR2. (c) YKL debris crop out along the road cut. A sharp transition between lower coarse-clast calcrete and upper thin-clast calcrete and the location of sample UR1 are highlighted. (d) Schematic cross-section across the OKL outcrop. OKL debris overlies a conglomerate bed ~100 m above the present Soreq stream. The location of sample UR4 is indicated. This figure is available in colour online at wileyonlinelibrary.com/journal/esp

younger generation reaches a thickness of up to ~10 m and was deposited at the current base level. Its flat top is cemented by thick, stage V calcrete. Relicts of similar conglomerates, which are situated at the same level, are found along the mountain-front down to the Soreq outlet. Two samples, from the top and base of the low and young conglomerate were collected (UR5 and UR6, respectively).

Alluvial terrace at the main Soreq stem (SAT) (35°117'E/31°757°N) A relict of a small alluvial terrace, 0.5–2 m thick, is exposed ~5 km upstream from the Ktalav landslides site (Figure 1). The terrace rises ~3 m above the present streambed. Formation of stage V calcrete over the conglomerate bed had contributed to its preservation. Two samples were collected from the center of the outcrop, ~50 m apart (UR10 and UR11).

Analytical Methods and Calcrete Dating

Dating the deposition of the colluvial and alluvial sediments at the study area is based on the age of formation of the pedogenic calcretes that have evolved on top of the various deposits (Sharp *et al.*, 2003). Therefore the ages are interpreted as an upper-limit to the time of deposition. Pedogenic calcrete form when calcium carbonate (CaCO₃) accumulates in soil horizons (Machette, 1985). Previous studies applied uranium series disequilibria (Sharp *et al.*, 2003; Candy *et al.*, 2004), radiocarbon dating (e.g. Amundson *et al.*, 1994), electron spin resonance (ESR) (Küçüküysal *et al.*, 2011) and cosmogenic chlorine-36 (³⁶Cl) (Liu *et al.*, 1994) to date the precipitation of CaCO₃ in calcretes. Forming near the surface, CaCO₃ minerals are inclined to dissolve and re-precipitate after the initial deposition, a process that may reset isotopic systems (Sharp *et al.*, 2003). Since

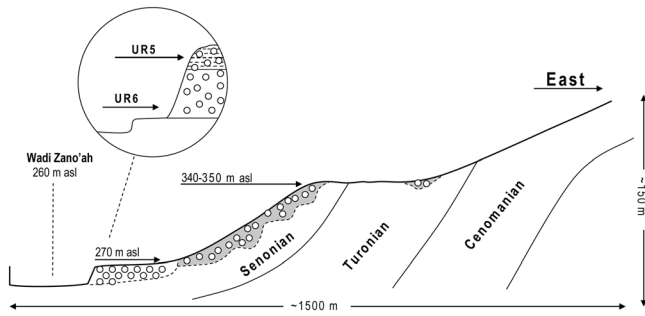


Figure 3. Schematic cross-section through the Judea Hill mountain front, east of Wadi Zano'ah (35°007'E/31°726'N). Two conglomerate units are present: the higher (older) one, marked by gray background, is cemented by massive calcrete and its original fan morphology has eroded. The lower (younger) one has a hard-pan calcrete evolved on the top of the outcrop (dashed lines texture), and its fan morphology is preserved. Location of samples UR5 and UR6 are indicated in the circular inset.

calcretes (and soils in general) are composed of both authigenic (*in situ* substrate) and non-authigenic sources such as dust, its isotopic initial values are hard to constrain (Amundson *et al.*, 1994).

Luminescence dating based on burial of the aeolian quartz grains can overcome these complexities. Aeolian transport is likely to result in the total bleaching of the optically stimulated luminescence (OSL) (Wintle, 2008) and thermally-transferred OSL (TT-OSL) signals in a quartz grain (Porat *et al.*, 2009). The burial process is expected to be simple: the growth of carbonate cement prevents the mixing of the soil and re-exposure of the quartz to sunlight. Hence, luminescence burial dating provides a robust upper limit age to the deposition of the substrate. Indeed, Shtober-Zisu *et al.* (2008) and Matmon *et al.* (2010) have successfully dated the formation of calcretes, in northern Israel, using OSL fast-signal measurements. In those cases the low dose rates of calcretes, 0.4–0.7 Gy ka⁻¹, and equivalent doses (De) values ~100–250 Gy, allowed the acquisition of reliable mid-Pleistocene ages.

Although OSL dating based on the fast component is widely accepted (Wintle, 2008), its buildup is usually saturated within a few 10⁵ yr. Furthermore, as the signal approaches saturation the uncertainty of the calculated age increases significantly. Recent studies explored the potential of the TT-OSL signal and found that it does not seem to be limited by saturation, and therefore may be applied to much older sediments (Wang *et al.*, 2006; Duller and Wintle, 2012). However, it was also recently suggested that the thermal stability of the TT-OSL signal may result in a significant underestimation of the ages and effectively limit this dating technique to the Pleistocene (Adamiec *et al.*, 2010; Shen *et al.*, 2011).

Many of the alluvial and colluvial sediments in the Soreq drainage have low dose rates and are potentially young enough to be dated by OSL. A limit to the number of samples stems from the low concentration of aeolian quartz fraction in the calcretes (usually less than 0.1% wt of the calcrete). Low quartz concentration required the sampling and dissolution of a few kilograms of calcrete for each sample, a considerable analytical effort indeed.

Sample collection, preparation for OSL and chemical analysis

Large calcrete samples (5–8 kg each) were collected to enable the extraction of sufficient quartz. Sample preparation and

measurements took place at the Geological Survey of Israel OSL dating laboratory. The outer centimeter of well-lithified samples that were collected in the daylight was removed in the dark using a steel-wire brush. Samples were then crushed using a jaw-crusher and placed in 10% hydrochloric acid (HCl). Samples UR5 and UR10 that were of loose sediments were collected into a light-tight bag under a blanket. Next, quartz grains of 74 to 150 µm size fraction were separated following the procedure described in Porat *et al.* (2007).

Representative portions of the samples (~0.5 kg) were pulverized, split, and dissolved. Their radioactive elements (uranium (U), potassium (K), thorium (Th)) content was analyzed for the calculation of α , β , and γ dose rates, with an ELAN DRC II 6000 ICP-MS at the Israel Geological Survey. The calcrete water content was assumed to be 5 ± 2% (Matmon *et al.*, 2010).

OSL and TT-OSL measurement and estimation of TT-OSL signal loss

For the OSL and TT-OSL measurements 2 mm and 5 mm aliquots were prepared, respectively. Both signals were measured with a Risø D-12 TL/OSL reader equipped with blue LED. Due to the expected antiquity of the samples and the long time needed for De determinations, only a small number of aliquots were measured for each sample. SAR protocols were adopted from Murray and Wintle (2000) and Porat *et al.* (2009) for the OSL and TT-OSL, respectively. TT-OSL was measured for all samples while OSL was also measured for the three samples from the YKL (samples UR1, UR2, and UR3). The comparison of the De values obtained by OSL and TT-OSL signals in the YKL samples established the reliability of the TT-OSL dating technique to the calcretized deposits. De values and their respective errors were calculated for each sample from the average and standard deviation of the aliquots De histogram using ANALYST software (Duller, 2007). Dose rates are obtained from radioactive element analysis and the attenuation factors (depth of burial, calcrete density, and water (H₂O) content) of the sediments and ages were calculated using DataBase software (from G.A.T. Duller, Aberystwyth University). The obtained TT-OSL ages are regarded as minimum for quartz burial, since they are expected to be affected by the thermal instability of the TT-signal (Adamiec *et al.*, 2010). Underestimation of the TT-OSL age due to the thermal instability of the TT-OSL traps depends on the true age of a sample and its surrounding temperature. Age corrections to the expected TT-OSL signal loss were calculated based on TT-OSL trap depth and frequency reported by Adamiec *et al.* (2010), and assuming a mean glacial–interglacial ambient temperature of 15°C (Affek *et al.*, 2008).

Results

Field descriptions, chemical data, and OSL ages of all samples are presented in Table I. Uncertainties of the TT-OSL based ages tend to be lower than the OSL's (with the exception of sample UR2). This difference is due to the fact that the OSL dose response curve (DRC) saturates and the natural signal is interpolated onto the sub-horizontal exponential + linear part of curve, resulting in large errors on the De (Figure 4a). However, the TT-OSL DRC is linear within the range of given doses (Figure 4b), and interpolation of the natural dose onto the curve produces smaller errors.

While the OSL ages are indistinguishable (within uncertainties) from one another at the YKL site, TT-signal dates show a hiatus

Table 1. Soreq drainage calcretes luminescence dating results

Sample	Site ¹	Depth(m)	Cosm ² ($\mu\text{Gy a}^{-1}$)	K (%)	U (ppm)	Th (ppm)	Ext. α ($\mu\text{Gy a}^{-1}$)	Ext. β ($\mu\text{Gy a}^{-1}$)	Ext. γ ($\mu\text{Gy a}^{-1}$)	Total dose ($\mu\text{Gy a}^{-1}$)	Number of aliquots	De ² (Gy)	Over- dispersion ³ (%)	Preliminary age (ka)	TT-OSL signal loss ⁴	Corrected TT-OSL age (ka)
UR1: OSL	YKL	3-3	140	0.16	0.8	0.8	3	225	158	526 ± 27	8/9	138 ± 31	24	263 ± 60	11%	354 ± 24
TT-OSL											7/7	169 ± 8	3	320 ± 22		
UR2: OSL	YKL	2-2	160	0.28	0.9	1.6	4	336	233	732 ± 33	9/9	176 ± 38	17	230 ± 52	10%	320 ± 43
TT-OSL											7/7	214 ± 27	10	292 ± 39		
UR3: OSL	YKL	0.2	243	0.25	0.8	1.5	3	301	211	759 ± 29	9/9	181 ± 36	19	239 ± 48	8%	257 ± 37
TT-OSL											7/7	181 ± 25	12	238 ± 34		
UR4: TT-OSL	OKL	4.1	128	0.12	0.5	0.3	2	149	95	373 ± 26	3/4	319 ± 75	19	845 ± 210	25%	1056 ± 262
UR5: TT-OSL	ZAF	0.2	243	0.07	0.5	0.8	2	128	106	479 ± 26	7/7	242 ± 20	7	506 ± 49	16%	587 ± 57
UR6: TT-OSL	ZAF	6.0	104	0.12	1.2	1.2	4	258	210	576 ± 25	7/7	335 ± 39	10	582 ± 73	18%	688 ± 86
UR10: TT-OSL	SAT	1.8	168	0.25	0.9	1.3	3	307	212	691 ± 30	9/9	169 ± 16	8	245 ± 25	8%	265 ± 27
UR11: TT-OSL	SAT	0.5	210	0.23	0.7	1.6	2	276	200	689 ± 29	9/9	156 ± 14	8	227 ± 23	8%	244 ± 25

Note: Location of the sampling sites can be found in Figure 1.

¹YKL, Young Ktalav landslide; OKL, Old Ktalav landslide; ZAF, Zano'ah alluvial fan; SAT, Soreq alluvial terrace.

²OSL De was obtained on 2 mm aliquots, and TT-OSL De was obtained on 8–9 mm aliquots.

³Over-dispersion indicates the intra-sample scatter.

⁴Signal loss was calculated following Adamiec et al. (2010), assuming ambient temperature of 15°C (Afek et al., 2008) and respective TT-OSL trap thermal lifetime of 1 to 4 Ma (Adamiec et al., 2010).

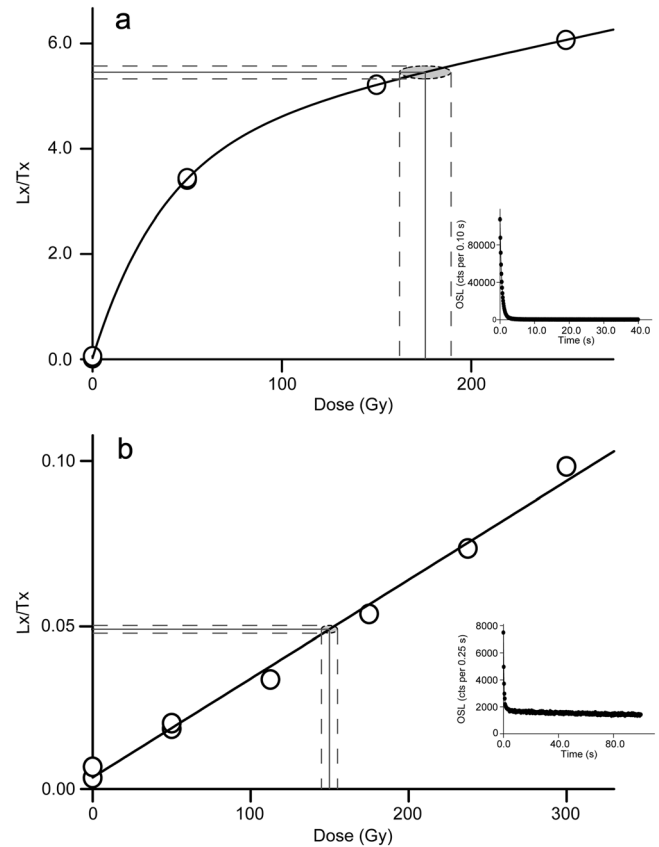


Figure 4. Typical dose response curves (DRCs) of OSL and TT-OSL signals of single aliquots of sample UR1. Insets present the signal decay over the measurement. The measured OSL and TT-OSL signals (L_x) are normalized to a fixed (10 Gy for OSL and 2.5 Gy for TT-OSL) test-dose to correct for potential sensitivity changes. Recycling ratio of both TT and OSL aliquots measured at 50 Gy were 0.99 and 1.07, respectively. (a) DRC for OSL equivalent dose (De). The normalized natural (marked with gray solid line) plots on the linear section of the curve which is considered to be less reliable and close to saturation; the overall uncertainty in De , marked by the dashed gray line translate to relatively large uncertainty of age. (b) DRC for TT-OSL De for one aliquot of sample UR1. The signal increases linearly and is not saturated in the tested irradiation range (0–300 Gy); the overall uncertainty in De , marked by the dashed gray line translates to relatively low uncertainty of age.

between samples UR1 and UR3 (Table I, see also figure DR4 in the online Supplementary Material). This hiatus is also expressed by the observed sharp transition between the lower, coarse-clast calcrete and the upper, thin-clast calcrete. It may reflect erosion that occurred between the main rock failure event that stabilized prior to 354 ± 24 ka and a shallower fine grain mass wasting event which stabilized after 354 ± 24 ka but before 257 ± 37 ka. Alternatively, the overall period defined by the two samples may result from a continuous process of calcretization, which lasted close to 100 ka. Either way, in the relatively low natural dose rates of the samples, TT-OSL based ages seem to be more reliable for the mid-Pleistocene samples. The two ages derived from the Zano'ah alluvial fan (ZAF) are the same within errors, though obviously the deposition of the conglomerate (sample UR6, 688 ± 86 ka) at the base of the fan predates its abandonment (sample UR5, 587 ± 57 ka).

The 'Old' Ktalav landslide (OKL) calcrete yielded a TT-OSL age of 1056 ± 262 ka. This age is in agreement with the 100 m higher base level at the time of slope failure of the OKL. With a De of only ~ 320 Gy and low dose rates (0.37 Gy ka^{-1}) due to deep overburden, this age is considered reliable. The two Soreq alluvial terrace (SAT) samples gave overlapping ages of 268 ± 27 and 244 ± 25 ka (samples UR9 and UR 10, respectively).

Discussion

Highly evolved calcretes and the absence of a typical scar and debris morphology are indicators for the relative antiquity of the landslide deposits in the Soreq drainage. These alluvial and colluvial sediments are circumstantially linked; frequent mass-wasting will ultimately lead to increased sediment supply from the slope to the drainage system, and force the accumulation of alluvial deposits at the mountain front; the position of many of these alluvial and colluvial deposits at the present base level associate them with a period which is defined between the end of the last significant incision and the stabilization of the slopes in the Soreq drainage.

The earlier descriptions of the present erosional mode (diffusion) and the past erosional mode (discrete mass wasting) constitute the two end members of erosion processes. A shift from one to the other requires a change in the conditions which control either hillslope gradient (such as stream incision) or potential triggers for slope failure (climatic, seismic, or anthropogenic). About one hundred thousand years are required to develop stage V calcrete cement (Machette, 1985; Candy *et al.*, 2004). Since all the investigated deposits are coated by such mature calcretes we conclude that the transition had to occur prior to ~100 ka, and that since then the slopes in the Soreq drainage are stable. During this minimum time of stability at least one inter-glacial–glacial cycle, as well as several major earthquakes at the adjacent DSR occurred (Amiran *et al.*, 1994; Kagan *et al.*, 2005). Hence, climatic changes and seismic events cannot be considered as limiting factors for significant landslide activity in the Judea Hills. It is therefore expected that the transition in hillslope erosion mode is the geomorphic response to decrease in incision rates of the Soreq; such decrease would have prevented the formation and maintenance of critical slope angles. Incision rates in the Soreq are likely to be controlled by rates and style of tectonic uplift.

The contrast between the present and the past erosional regimes suggests that the Soreq hillslope erosion mode changed from a mode of high landslide-frequency, high sediment flux, and alluvial deposit buildup, to the current dissolution-controlled erosion with low sediment flux. Therefore, the dating of alluvial and colluvial sediment deposited at the present streambed provides a measure of the timescale of geomorphic response to the termination, or significant decrease, in tectonic uplift, and gives an upper limit to the last significant uplift phase of the Judea Hills. The dating of deposits that mark higher (and older) base levels, such as the landslide that terminates ~100 m above the present active stream, constrains the amount and rate of incision and uplift prior to the stabilization of the present streambed.

All the obtained ages are older than 244 ± 25 ka. These ages are in agreement with the field observations in which stage V calcretes coat all investigated and dated geomorphic features suggesting mid-Pleistocene stabilization as a result of decrease in stream incision and the stabilization of the present base level.

Tectonic implications of OKL dating

Apart from the OKL that was deposited ~100 m above the present streambed, all other investigated deposits accumulated at the present base level. Hence, incision of ~100 m occurred later than 1056 ± 262 ka and prior to the deposition of the ZAF at the present streambed at 688 ± 86 ka. These ages imply an incision rate of 270 m Ma^{-1} , an order of magnitude greater than CaCO_3 dissolution rates that were measured in the Judea

Hills (Haviv *et al.*, 2006) and other Mediterranean carbonate terrains (Gabrovšek, 2009, and references cited therein). Stream incision preference over the rate of the CaCO_3 dissolution means that hillslope retreat through CaCO_3 dissolution could not have kept pace with the base level lowering. This led to the formation of critical slopes, and hillslope erosion was controlled by landslides. In contrast, since 688 ± 86 ka, incision of the Soreq and its tributaries has been negligible, suggesting significant loss of runoff water into the karstic system and a major decrease in stream power. For example, in a single, rare rainfall event during late February of 2009, ~200 mm (40% of the overall annual average) had dropped within 48 hours. Nevertheless, no flooding and or mass-wasting were reported in the Soreq system and its natural hillslopes. This suggestion is also supported by several field observations: (1) nearly all longitudinal stream profiles of small tributaries of the Soreq are not concave (which would have indicated that they reached steady state), (2) the preservation of zones of increased stream gradient in these streams (Figure 5, profiles of stream gradient are available in the online Supplementary Material, item DR5) and, (3) the preservation of steep linear hillslopes. These field phenomena indicate the lack of surface runoff and the present low stream power on the slopes and channels of the Judea Hills.

The projection of the active stream profile of the Soreq drainage intersects the profiles of the adjacent interfluvies at the coastal plain indicating that downstream from this intersection point, stream incision gives way to alluvial and coastal deposition (Figure 6). We therefore interpret this point to be in equilibrium with its base level and, respectively, it had experienced zero vertical movements during the Pleistocene. Assuming that the Pleistocene uplift of the Judea Hills occurred through regional westward tilting, we refer to this point as the 'hinge' of the Judea Hills tilt (Figure 6). In order to achieve 100 m of uplift and incision to the present streambed, 20 km east of the hinge, only 0.3° westward tilt is required from the early Pleistocene to 688 ± 86 ka. This calculation agrees with previous studies which attribute 200–400 m of uplift of the Judea Hills to a $< 1^\circ$ westward tilting phase that commenced in the late Pliocene (Begin and Zilberman, 1997; Bar, 2009) and then followed by incision of the Soreq drainage to its current level. Early Pleistocene uplift of the western rim of the DSR through arching also led to incision and re-organization of drainage systems in northern and southern Israel (Matmon *et al.*, 1999; Guralnik *et al.*, 2010).

Landslide frequency during the transitions from mass wasting to stable slopes

The sampled sites at the present streambed were selected to represent different levels of landslide frequencies during the transition from mass-wasting to diffusive erosion. Deposition of alluvial fans at the mountain front is expected to occur when high flux of sediments is delivered from the slopes to the drainage system due to frequent landslides. Incision of the Zano'ah tributary into the fan sediments became possible when the flux of sediment decreased. Therefore, between the accumulation of the sediment at the base of the fan outcrop (sample UR5; 688 ± 86 ka) and the abandonment of the top of the fan (sample UR6; 587 ± 57 ka), sediment flux, and by inference, landslides frequency in the Zano'ah tributary decreased dramatically. The YKL is one of few (six out of total 37) which reached the present streambed that has recognizable scar morphology and may represent one of the youngest

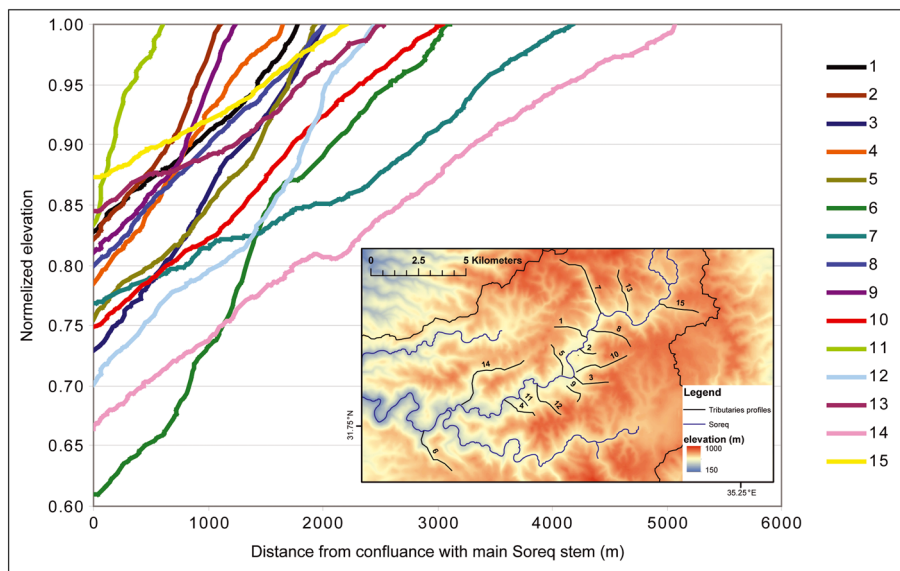


Figure 5. Elevation profiles of 15 of the Soreq tributaries. Elevations were normalized to the maximum elevation of each profile. Nearly all profiles are not concave and contain zones of increased stream gradient that are not controlled by lithology (profiles of stream gradient are available in the online Supplementary Material, item DR4). Inset in the lower right shows the location of the profiles. Profiles were extracted from a 25 m pixel digital elevation model (DEM) using the geographic information system (GIS) hydrology tool, and smoothed by a moving average over a 250 m wide window. Map was plotted using ITM projection. This figure is available in colour online at wileyonlinelibrary.com/journal/espl

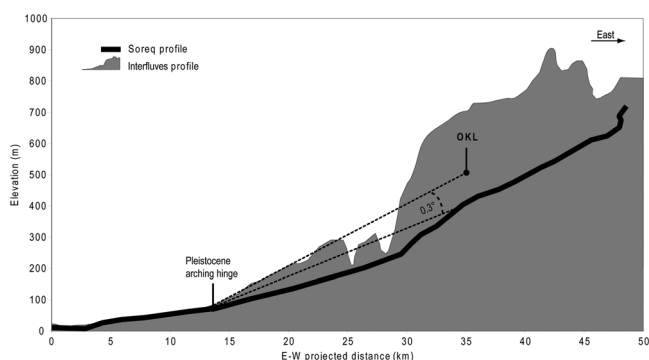


Figure 6. Elevation profiles of the northern branch of the Soreq stream (black) and adjacent interfluvies (gray) from the main Judea Hills water divide to the Mediterranean Sea (see Figure 1 for location). The dashed line connects the Pleistocene arching hinge with the early-mid Pleistocene OKL base level and with the present stream right below it. Westward tilt of 0.3° can explain the ~ 100 m mid-Pleistocene incision observed at the OKL. See section text for details.

landslides that occurred in the Judea Hills, possibly during a period of relatively low landslide frequency. Stable base level can generally enable a limited number of landslides to occur; assuming that all six 'Young' landslides occurred around the same time of the YKL (354 ± 24 ka), and that the other 31 landslides that lack morphologic features occurred prior to the YKL but after the establishment of the base level at 688 ± 86 ka, the landslide frequency had dropped gradually to $\sim 20\%$ within ~ 330 ka. Since landslides that lack morphologic features and reach the present streambed can be identified only along road-cuts, it is likely that a number of them were left unmapped and as a consequence uncounted. Therefore the 330 ka should be regarded as a maximum period for 80% decrease in landslide frequency.

Figure 7 summarizes the possible temporal framework for the major decrease in the Soreq drainage landslide frequency from middle to late Pleistocene. The slopes of the Soreq drainage enabled relatively high frequency of landslides and sediment flux before and during the accumulation of the ZAF at

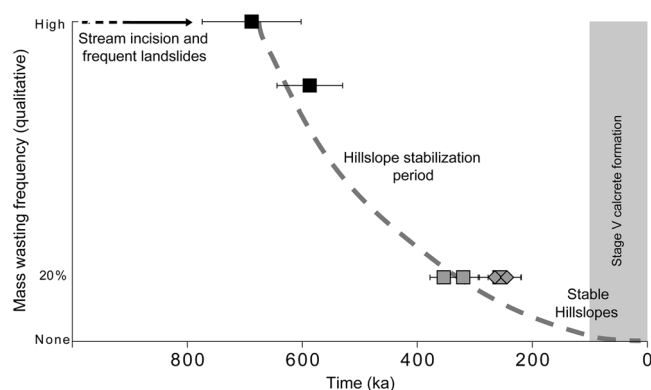


Figure 7. Interpretation of alluvial and colluvial TT-OSL ages in terms of relative landslide frequency. ZAF samples are marked with black squares, YKL samples are marked with gray squares, samples from SAT are marked with gray diamonds, and the minimum time required for stage V calcrete to develop is marked by a gray rectangular. Dashed gray arrow across the stabilization period is one possible landslides decay curve; gradual decay of landslide frequency was observed by Densmore *et al.* (1998), see text for more details.

688 ± 86 ka. Shortly after, landslide frequency decreased, leading to lower sediment fluxes and the abandonment of alluvial fans at the Judea Hills mountains front at 587 ± 57 ka. The frequency of landslides continued to decrease, although a few landslides still occurred as evidenced by the YKL at 354 ± 24 ka. Finally, the hillslopes in the Soreq drainage stabilized and diffusive erosion became dominant, at least ~ 100 ka before the present. Thus, the stabilization period of the drainage hillslopes lasted a minimum of 330 ka (if we assume the YKL to be the last one) and a maximum of 580 ka (since stage V calcretes require ~ 100 ka to develop) (Figure 7). This period of relaxation which is calculated based on our field observations and TT-OSL dating agrees well with the results of numerical modeling; Densmore *et al.* (1998) predicted that an abrupt cease in uplift activity will be followed by gradual decay of landslide frequency due to progressive cession in stream incision and the onset of aggradation throughout the drainage.

Their model employed physical parameters typical to the Basin and Range province, and predicted that a 90% decrease in landslide activity will occur ~100 ka after uplift had ceased, in the order of our results.

Gradual transition from landslide-controlled to dissolution-controlled hillslope erosion, as documented in the Soreq drainage, reflects the hillslope response to dramatic weakening, or cessation, of stream incision. Such a response is expected to follow stabilization of the base level at the piedmont, rather than distal base level stabilization (the Mediterranean coast is located ~40 km west to the Judea Hills mountain front) (Frankel and Pazzaglia, 2006). It is suggested that weakening of tectonic uplift rate led to decrease in stream incision to a rate that is lower than the erosive capacity of carbonate dissolution in the Judea Hills. At that point carbonate dissolution of the hillslopes kept pace with stream incision and prevented the development of critical slopes. The period of 330 to 580 ka between the high landslides frequency to the stabilization of the hillslopes may include a gradual weakening of the uplift. However, the gradual decrease in landslide activity can be explained simply by the time in which the geomorphic signal of base-level stabilization traveled across the drainage, supporting the model presented by Densmore *et al.* (1998).

We demonstrate that colluvial deposits may be used as markers for stream incision and base level stabilization, much like alluvial deposits that are commonly used for this purpose. The geomorphic response of hillslopes can be translated to phases of tectonic uplift or quiescence based on the colluvial deposit archive. The research of colluvial deposits will enable future studies to expand to regions that do not preserve alluvial deposits and therefore were left unstudied. Our study can be regarded as a natural experiment in which the landscape responded to a change in tectonic forcing by a change in the character of slope erosion (Tucker and Hancock, 2010).

Conclusions

Combining field observations and TT-OSL dating of alluvial and colluvial deposits in the Soreq drainage we find the following. (1) Incision of ~100 m occurred from 1056 ± 265 to 688 ± 86 ka due to ~0.3° westward tilt of the Judea Hills; such incision invoked high frequency of landslide activity in the drainage and, as a result the deposition of alluvial terraces and fans. (2) Present base level was established after 688 ± 86 ka, and hillslopes gradually stabilized as a response to a cease or dramatic weakening of the uplift. This process led to a dramatic decrease in the flux of coarse sediment in the Soreq drainage and the abandonment of alluvial fans at the mountain front. By the time the YKL occurred (354 ± 24 ka), landslide frequency dropped below 20%; overall hillslope stabilization period lasted 330–580 ka. (3) The Soreq drainage has been stable for at least 100 ka and possibly since the YKL occurred; preservation of non-concave stream and hillslope profiles is hence attributed to the lack of sufficient stream-power due to the loss of runoff water into the karstic system.

Acknowledgments—The authors wish to acknowledge Grzegorz Adamiec for his help with the TT-OSL age calculations, to Yakov Weiss and Tamar Ryb that have assisted in the field, and to Lisa S. Walsh and three anonymous reviewers for their critical review. This study was funded by the Israel Science Foundation grant ISF 50/10.

Supporting Information

Supporting information may be found in the online version of this article.

References

- Adamiec G, Duller GAT, Roberts HM, Wintle AG. 2010. Improving the TT-OSL SAR protocol through source trap characterisation. *Radiation Measurements* **45**: 768–777. DOI: 10.1088/0022-3727/41/13/135503
- Affek HP, Bar-Matthews M, Ayalon A, Matthews A, Eiler JM. 2008. Glacial/interglacial temperature variations in Soreq cave speleothems as recorded by 'clumped isotope' thermometry. *Geochimica et Cosmochimica Acta* **72**: 5351–5360. DOI: 10.1016/j.gca.2008.06.031
- Amiran DHK, Arie E, Turcotte T. 1994. Earthquakes in Israel and adjacent areas – macroseismic observations since 100 BCE. *Israel Exploration Journal* **44**: 260–305.
- Amundson R, Wang Y, Chadwick O, Trumbore S, Mcfadden L, McDonald E, Wells S, Deniro M. 1994. Factors and processes governing the C-14 content of carbonate in desert soils. *Earth and Planetary Science Letters* **125**: 385–405.
- Ayalon A, Bar-Matthews M, Sass E. 1998. Rainfall–recharge relationships within a karstic terrain in the eastern Mediterranean semi-arid region, Israel: delta O-18 and delta D characteristics. *Journal of Hydrology* **207**: 18–31.
- Bar O. 2009. The Shaping of the Continental Margin of Central Israel Since the Late Eocene – Tectonics, Morphology and Stratigraphy PhD thesis. Ben-Gurion University of the Negev: Beer-Sheva; 212.
- Begin ZB, Zilberman E. 1997. Main Stages and Rate of the Relief Development in Israel, Geological Survey of Israel, Report No. GSI/24/97. Israel Geological Survey: Jerusalem; 63.
- Bentor YK, Vroman A, Zak I. 1965. Geological Map of Israel, Southern Sheet. 1:250000. Israel Geological Survey: Jerusalem.
- Bigi A, Hasbargen LE, Montanari A, Paola C. 2006. Knickpoints and hillslope failures: interactions in a steady-state experimental landscape. In *Tectonics, Climate, and Landscape Evolution*, Willett SD, Hovius N, Brandon MT, Fisher DM (eds), Geological Society of America Special Paper. Geological Society of America: Boulder, CO; 295–307. DOI: 10.1130/2006.2398(18)
- Binnie SA, Phillips WM, Summerfield MA, Fifield LK. 2007. Tectonic uplift, threshold hillslopes, and denudation rates in a developing mountain range. *Geology* **35**: 743–746. DOI: 10.1130/G23641A.1
- Bloom AL. 1998. *Geomorphology*. Prentice Hall: Englewood Cliffs, NJ; 482.
- Brown ET, Stallard RF, Larsen MC, Raisbeck GM, Yiou F. 1995. Denudation rates determined from the accumulation of in situ-produced Be-10 in the Luquillo experimental forest, Puerto-Rico. *Earth and Planetary Science Letters* **129**: 193–202.
- Buchbinder B, Calvo R, Siman-Tov R. 2005. The Oligocene in Israel: a marine realm with intermittent denudation accompanied by mass-flow deposition. *Israel Journal of Earth Sciences* **54**: 63–85.
- Burbank DW, Leland J, Fielding E, Anderson RS, Brozovic N, Reid MR, Duncan C. 1996. Bedrock incision, rock uplift and threshold hillslopes in the northwestern Himalayas. *Nature* **379**: 505–510.
- Candy I, Black S, Sellwood BW. 2004. Quantifying time scales of pedogenic calcrete formation using U-series disequilibria. *Sedimentary Geology* **170**: 177–187. DOI: 10.1016/j.sedgeo.2004.07.003
- Densmore AL, Ellis MA, Anderson RS. 1998. Landsliding and the evolution of normal-fault-bounded mountains. *Journal of Geophysical Research – Solid Earth* **103**: 15203–15219.
- Duller GAT. 2007. *Analyst 3.24*. University of Wales: Newport.
- Duller GAT, Wintle AG. 2012. A review of the thermally transferred optically stimulated luminescence signal from quartz for dating sediments. *Quaternary Geochronology* **7**: 6–20. DOI: 10.1016/j.quageo.2011.09.003
- Ford D, Williams PW. 2007. *Karst Geomorphology and Hydrology*. John Wiley & Sons: Chichester.
- Frankel KL, Pazzaglia FJ. 2006. Mountain fronts, base level fall, and landscape evolution insights from the southern Rocky Mountains. In *Tectonics, Climate, and Landscape Evolution*, Willett SD, Hovius N, Brandon MT, Fisher DM (eds). Geological Society of America: Boulder, CO; 419–434. DOI: 10.1130/2006.2398(26)
- Gabrovšek F. 2009. On concepts and methods for the estimation of dissolutional denudation rates in karst areas. *Geomorphology* **106**: 9–14. DOI: 10.1016/j.geomorph.2008.09.008
- Guralnik B, Matmon A, Avni Y, Fink D. 2010. Be-10 exposure ages of ancient desert pavements reveal Quaternary evolution of the Dead

- Sea drainage basin and rift margin tilting. *Earth and Planetary Science Letters* **290**: 132–141. DOI: 10.1016/j.epsl.2009.12.012
- Haviv I, Enzel Y, Zilberman E, Whipple K, Stone J, Matmon A, Fifield LK. 2006. Climatic control on erosion rates of dolomite limestone hilltops, Annual Meeting. The Israel Geological Society: Bet-Shean; 54.
- Heimsath AM, Chappell J, Spooner NA, Quetiaux DG. 2002. Creeping soil. *Geology* **30**: 111–114. DOI: 10.1130/0091-7613(2002)030<0111:CS>2.0.CO;2
- Hovius N. 1998. Controls on sediment supply by large rivers. In *Relative Role of Eustasy, Climate and Tectonics in Continental Rocks*, Shanley KW, McCabe PJ (eds), SEPM special publication. Society for Sedimentary Geology: Tulsa, OK; 1–16.
- Iverson RM. 2000. Landslide triggering by rain infiltration. *Water Resources Research* **36**: 1897–1910. DOI: 10.1029/2000WR900090
- Kagan EJ, Agnon A, Bar-Matthews M, Ayalon A. 2005. Dating large infrequent earthquakes by damaged cave deposits. *Geology* **33**: 261–264. DOI: 10.1130/G21193.1
- Keefer DK. 1994. The importance of earthquake-induced landslides to long-term slope erosion and slope-failure hazards in seismically active regions. *Geomorphology* **10**: 265–284.
- Kirchner JW, Finkel RC, Riebe CS, Granger DE, Clayton JL, King JG, Megahan WF. 2001. Mountain erosion over 10 yr, 10 kyr, and 10 myr time scales. *Geology* **29**: 591–594. DOI: 10.1130/0091-7613(2001)029<0591:MEQYK>2.0.CO;2
- Küçüküysal C, Engin B, Turkmenoglu AG, Aydas C. 2011. ESR dating of calcrite nodules from Bala, Ankara (Turkey): preliminary results. *Applied Radiation and Isotopes* **69**: 492–499. DOI: 10.1016/j.apradiso.2010.10.005
- Liu BL, Phillips FM, Elmore D, Sharma P. 1994. Depth dependence of soil carbonate accumulation based on cosmogenic ^{14}C dating. *Geology* **22**: 1071–1074.
- Machette MN. 1985. Calcic soils of the southwestern United States. In *Soils and Quaternary Geology of the Southwestern United States*, Weide DL (ed.). Geological Society of America: Boulder, CO; 1–21.
- Matmon A, Enzel Y, Zilberman E, Heimann A. 1999. Late Pliocene and Pleistocene reversal of drainage systems in northern Israel: tectonic implications. *Geomorphology* **28**: 43–59.
- Matmon A, Katz O, Shaar R, Ron H, Porat N, Agnon A. 2010. Timing of relay ramp growth and normal fault linkage, Upper Galilee, northern Israel. *Tectonics* **29**: 1–13. DOI: 10.1029/2009TC002510
- Montgomery DR, Brandon MT. 2002. Topographic controls on erosion rates in tectonically active mountain ranges. *Earth and Planetary Science Letters* **201**: 481–489. DOI: 10.1016/S0012-821X(02)00725-2
- Murray AS, Wintle AG. 2000. Luminescence dating of quartz using an improved single-aliquot regenerative-dose protocol. *Radiation Measurements* **32**: 57–73. DOI: 10.1016/S1350-4487(99)00253-X
- Nir D. 1989. *The Geomorphology of Israel*. Academ, New Edition: Jerusalem (in Hebrew).
- Porat N, Duller GAT, Roberts HM, Wintle AG. 2009. A simplified SAR protocol for TT-OSL. *Radiation Measurements* **44**: 538–542. DOI: 10.1016/j.radmeas.2008.12.004
- Porat N, Levi T, Weinberger R. 2007. Possible resetting of quartz OSL signals during earthquakes – evidence from late Pleistocene injection dikes, Dead Sea basin, Israel. *Quaternary Geochronology* **2**: 272–277. DOI: 10.1016/j.quageo.2006.05.021
- Roering JJ, Kirchner JW, Sklar LS, Dietrich WE. 2001. Hillslope evolution by nonlinear creep and landsliding: an experimental study. *Geology* **29**: 143–146. DOI: 10.1130/0091-7613(2001)029<0143:HEBNCA>2.0.CO;2
- Saas E, Bein A. 1978. Platform Carbonates and Reefs in the Judea Hills, Carmel, and Galilee, The International Congress of Sedimentology Guide Book. The International Congress of Sedimentology: Jerusalem; 241–276.
- Sharp WD, Ludwig KR, Chadwick OA, Amundson R, Glaser LL. 2003. Dating fluvial terraces by Th-230/U on pedogenic carbonate, Wind River Basin, Wyoming. *Quaternary Research* **59**: 139–150. DOI: 10.1016/S0033-5894(03)00003-6
- Shatner Y. 1957. The morphology of the Jerusalem Mountains, Judea and Jerusalem. *The Israel Research Society* **1**: 137–143 (in Hebrew).
- Shen ZX, Mauz B, Lang A. 2011. Source-trap characterization of the thermally transferred OSL in quartz. *Journal of Physics D: Applied Physics* **44**: 1–12. DOI: 10.1088/0022-3727/44/29/295405
- Shtober-Zisu N, Greenbaum N, Inbar M, Flexer A. 2008. Morphometric and geomorphic approaches for assessment of tectonic activity, Dead Sea Rift (Israel). *Geomorphology* **102**: 93–104. DOI: 10.1016/j.geomorph.2007.06.017
- Sneh A, Buchbinder B. 1984. Miocene to Pleistocene Surfaces and their Associated Sediments in the Shefela Region, Israel, Israel Geological Survey, Current Research 1983–1984. Israel Geological Survey: Jerusalem; 60–64.
- Tucker GE, Hancock GR. 2010. Modelling landscape evolution. *Earth Surface Processes and Landforms* **35**: 28–50. DOI: 10.1002/esp.1952
- Wang XL, Lu YC, Wintle AG. 2006. Recuperated OSL dating of fine-grained quartz in Chinese loess. *Quaternary Geochronology* **1**: 89–100. DOI: 10.1016/j.quageo.2006.05.020
- Wdowinski S, Zilberman E. 1996. Kinematic modelling of large-scale structural asymmetry across the Dead Sea Rift. *Tectonophysics* **266**: 187–201.
- Wdowinski S, Zilberman E. 1997. Systematic analyses of the large-scale topography and structure across the Dead Sea Rift. *Tectonics* **16**: 409–424.
- Wintle AG. 2008. Luminescence dating: where it has been and where it is going. *Boreas* **37**: 471–482. DOI: 10.1111/j.1502-3885.2008.00059.x
- Wondzell SM, King JG. 2003. Postfire erosional processes in the Pacific Northwest and Rocky Mountain regions. *Forest Ecology and Management* **178**: 75–87. DOI: 10.1016/S0378-1127(03)00054-9